Journal of Alloys and Compounds 586 (2014) 475–478

Contents lists available at ScienceDirect

Journal of Alloys and Compounds

journal homepage: www.elsevier.com/locate/jalcom

ARXPS and DFT studies of thermally induced Pb surface segregation on Au/Cu alloys

Edgar Völker [a,b,1], Federico J. Williams [b,*], Timo Jacob [c], David J. Schiffrin [a]

[a] Chemistry Department, University of Liverpool, Liverpool L69 7ZD, United Kingdom
[b] Departamento de Química Inorgánica, Analítica y Química Física, INQUIMAE-CONICET, Facultad Ciencias Exactas y Naturales, Universidad de Buenos Aires, Buenos Aires C1428EHA, Argentina
[c] Institute of Electrochemistry, Ulm University, Albert-Einstein-Allee 47, D-89081 Ulm, Germany

ARTICLE INFO

Article history:
Received 26 August 2013
Received in revised form 8 October 2013
Accepted 15 October 2013
Available online 24 October 2013

Keywords:
Metals and alloys
Photoelectron spectroscopies
XPS
DFT
Gold–copper alloy

ABSTRACT

Surface segregation of Pb has been studied using angle resolved X-ray Photoelectron Spectroscopy (ARXPS) and Density Functional Theory (DFT) modelling in a polycrystalline $Au_{0.85}Cu_{0.15}$ alloy. Au surface enrichment was found in the alloy surface, whereas Pb surface enrichment was detected after annealing. ARXPS depth profiles show a 23% surface coverage by Pb atoms. DFT calculations predict an approximate coverage of ¼ monolayer (ML) of Pb atoms in the first atomic layer, consistent with the experimental results. The results presented here are an example of the importance of low concentration of impurities in determining the surface composition of bulk alloys.

1. Introduction

The composition of an electrode surface is a determining factor in the course of electrocatalytic reactions. It is well established now that both the environment surrounding an electrode and the applied potential can greatly influence its surface composition [1,2], thus leading to radically different electrocatalytic behaviour. Equally important, metal impurities in the electrode material can also have a large influence on surface reactions. Since sample annealing is commonly employed for the preparation of bimetallic alloy nanoparticles as a means of stabilizing their configuration, it is important to understand the driving force of segregation phenomena to predict if very low concentrations of impurities could affect their surface composition by annealing.

Bimetallic alloys are of great interest in electrocatalysis because they offer a way to fine tune their catalytic properties and make them more active as compared to their simple component counterparts [3,4]. This depends on surface composition, which can differ significantly from that in the bulk because of differences in surface segregation energies of the alloy constituents. It was recently shown [5] that for the Au–Cu system the surface is preferentially enriched with Au atoms; whereas when exposed to an atmosphere of O_2, a surface inversion repopulation takes place, with the surface becoming enriched with Cu atoms thus favouring O adsorption. Thus, during the course of (electro-)catalytic reactions, alloy systems might not remain rigid, but may change their surface composition according to the environment in which they are placed [6]. In addition, it was found that Pb impurities diffused to the surface when the sample was annealed and this observation triggered the present study.

Segregation of Pb can have a deleterious effect on catalytic performance due to the blocking of active sites. Thus, impurities that are present in low concentration could have a profound effect in catalyst performance. The present work shows the use of DFT calculations to rationalize segregation phenomena of importance in catalysis, and how this behaviour can be radically different in bulk and nanoparticle alloy systems [7]. Angle resolved X-ray Photoelectron Spectroscopy (ARXPS) measurements on a $Au_{0.85}Cu_{0.15}$ alloy and Density Functional Theory (DFT) calculations were performed to study the effect of surface segregation of Pb impurities after sample annealing. A comparison between nanoparticulate materials and bulk is made and it is shown that very low concentrations of Pb impurities affect the bulk systems while leaving the nanoparticulate systems unaffected.

* Corresponding author. Address: Departamento de Química Inorgánica, Analítica y Química-Física, INQUIMAE-CONICET, Facultad Ciencias Exactas y Naturales, Pabellón 2, Ciudad Universitaria, Buenos Aires C1428EHA, Argentina. Tel.: +54 11 45763380x105.
E-mail address: fwilliams@qi.fcen.uba.ar (F.J. Williams).
[1] Present address: DQIAyQF, INQUIMAE-CONICET, Facultad Ciencias Exactas y Naturales, Pabellón 2, Ciudad Universitaria, Buenos Aires C1428EHA, Argentina.

0925-8388/$ - see front matter © 2013 Elsevier B.V. All rights reserved.
http://dx.doi.org/10.1016/j.jallcom.2013.10.119

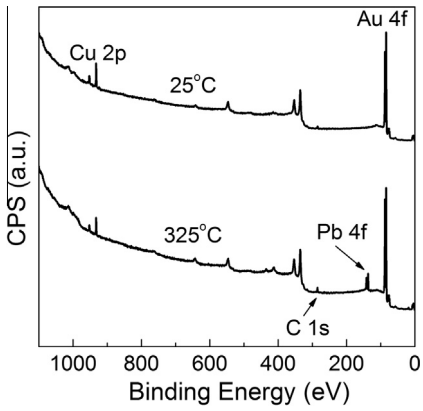

Fig. 1. XPS survey scans for a $Au_{0.85}Cu_{0.15}$ alloy after Ar^+ sputtering. 25 °C: no annealing; 325 °C: after annealing for 1 h.

2. Material and methods

Sample preparation and surface treatment have been described in more detail elsewhere [5]. In short, the base metals (Au (99.9985%) and Cu (99.999%) Alfa Aesar UK) were placed in a tube furnace under H_2/Ar atmosphere at 1100 °C for 6 h. The $Au_{0.85}Cu_{0.15}$ alloy studied was polished with increasingly fine alumina slurries to a mirror finish. It was characterised by XRD (PANalytical X'pert PRO Multi-Purpose Diffractometer, Co $K\alpha_1$ radiation), to ensure that the alloy was formed [5]. X-ray Photoelectron Spectroscopy measurements (XPS) were performed under UHV conditions (base pressure < 5×10^{-10} mbar) in a SPECS spectrometer system equipped with a 150 mm mean radius hemispherical electron energy analyzer and a nine channeltron detector. XPS spectra were acquired at a constant pass energy of 20 eV using an un-monochromated MgKα (1253.6 eV) source operated at 12.5 kV and 20 mA and a detection angle of 30° with respect to the sample normal on grounded conducting substrates. The binding energies quoted are referred to the Au $4f_{7/2}$ emission at 84.0 eV. The surface concentration of Pb was determined by angle resolved XPS (ARXPS) [5]. Sample heating inside the XPS analysis chamber was achieved by electron bombardment, temperature was measured with a chromel–alumel (type K) thermocouple spot welded to the side of the alloy. All ARXPS experiments were performed at room temperature (25 °C). The annealing time was 1 h, and then the sample was allowed to cool to ambient temperature before ARXPS measurements.

3. Calculations

All first-principles calculations of surface segregation properties of lead were performed with the CASTEP (Cambridge Serial Total Energy Package) code [8] that implements density functional theory (DFT) using plane-wave pseudopotentials. The core electrons for all atoms, were replaced by Vanderbilt ultrasoft pseudopotentials [9] and the exchange–correlation energies were evaluated with the PBE-form of the generalized-gradient approximation (GGA). A plane-wave basis set with an energy cut-off of 380 eV was used for all surfaces. The Brillouin zones of the (1×1)-surface unit cells were sampled with (4×4) Monkhorst–Pack k-point meshes. These surfaces were represented by 5-layer slabs, where periodic images were separated by a vacuum of at least 13 Å. During the geometry optimizations the bottom two layers were fixed at the calculated bulk structure and the geometry of the remaining layers (plus adsorbates) was fully optimised up to <0.01 eV/Å. Different coverages were studied by using (1×1), (2×2), and (3×3) surface unit cells.

4. Results and discussion

Fig. 1 shows XPS survey scans for a $Au_{0.85}Cu_{0.15}$ alloy after Ar^+ etching followed by annealing for 1 h in UHV at 325 °C.

Only Au and Cu signals are observed before sample annealing. However after annealing Pb 4f signals are clearly visible, although high purity base metals were employed. The ARXPS results for Pb are presented in Fig. 2. The binding energy for Pb $4f_{7/2}$ is 136.9 eV, in excellent agreement with literature data of 136.8 eV [10].

No other signals from metals besides those of Au and Cu are present, although some small C 1s signal can be seen. This is absent in the sample before annealing and can be attributed to deeply buried contamination in the constituent metals that diffuses at higher temperatures. Pb was not observed for any of the other alloys previously studied at lower temperatures [5]. The Pb 4f signal increase with detection angle indicates that Pb is specifically adsorbed at the surface. The concentration profiles for the $Au_{0.85}Cu_{0.15}$ alloy before and after annealing were calculated using a concentration gradient model with maximum entropy regularisation (Fig. 3) [11,12].

Fig. 3a shows that, before annealing, the alloy surface is enriched in Au and as expected, the concentration profiles tend to their bulk values as depth increases. Fig. 3b shows that after annealing diffusion of Pb to the surface changes the atomic distribution depth with a clear enrichment of Pb and the concomitant decrease of the Au and Cu surface concentrations.

Pb transport to the surface would be expected to be a diffusional controlled process and it is interesting to model the resulting surface coverage in order to compare with the XPS and DFT results (see later). This was calculated assuming that adsorption is an irreversible process and therefore, it can be calculated from the integrated Fick's first law for linear diffusion [13]:

$$\Gamma(t) = 2D^{1/2}c^{b}t^{1/2}\pi^{-1/2} \quad (1)$$

$\Gamma(t)$ is the surface concentration of Pb, t is the time, D the diffusion coefficient of Pb atoms in the alloy and C^b is the bulk concentration of Pb.

Eq. (1) assumes that there is no change in the activity coefficient of Pb with distance and therefore, the value of D is uniform in all the material and also that there are no additional contributions to the diffusion rate, for instance, due to the formation of intermetallics or separate phase formation. Temperature dependence of the solid state diffusion of Pb in Au was investigated by Schopper [14] between 20 and 100 °C employing an optical technique. It was found that diffusion of Pb could be regarded as an activated process with a diffusion coefficient given by:

$$D = (0.016 + 0.005)\ \mathrm{cm^2\ s^{-1}} \times \exp(-E_{act}/RT) \quad (2)$$

where E_{act} is the activation energy for diffusion, R is the gas constant and T is the absolute temperature. A value of $E_{act} = 71 \pm 8$ kJ mol^{-1} was found and from Eq. (2), the diffusion coefficient of Pb in Au at 598 K is approximately $D_{598} = 9.8 \times 10^{-9}$ cm^2 s^{-1}. With the exception of a single gravimetric measurement at 100 °C by

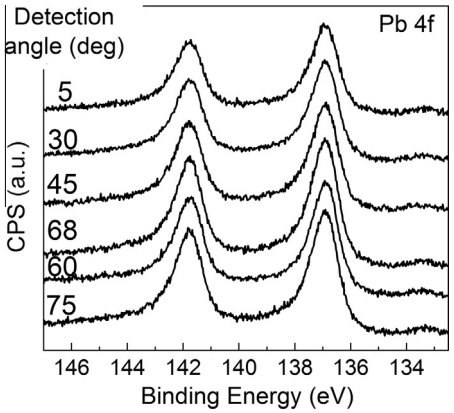

Fig. 2. Pb XP signal for a $Au_{0.85}Cu_{0.15}$ alloy after annealing for 1 h at 325 °C.

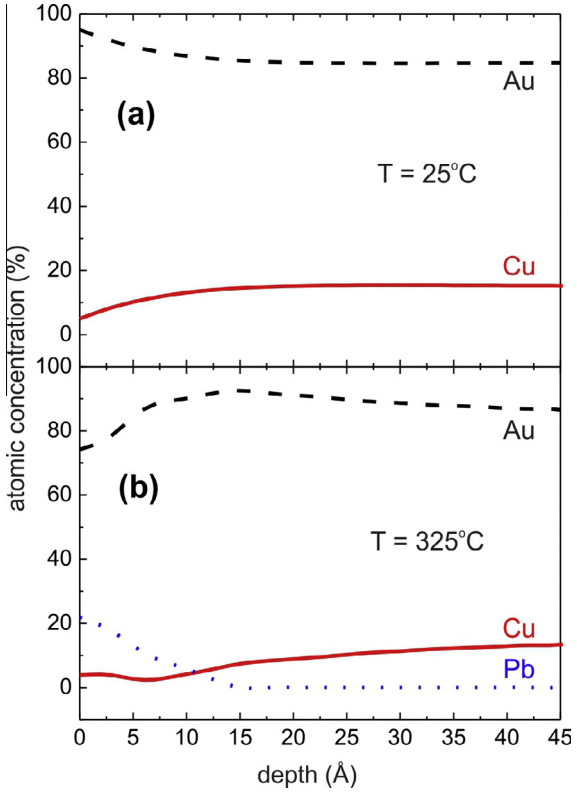

Fig. 3. Concentration profiles for Cu (solid line), Au (dashed line) and Pb (dotted line) for a $Au_{0.85}Cu_{0.15}$ alloy before (a) and after annealing at 325 °C (b).

Leidheiser [15], no other reliable data for the diffusion coefficient of Pb could be found in the literature. This work reported $D_{373} = 1.6 \times 10^{-12}$ cm^2 s^{-1}, in good agreement with the value calculated from Eq. (2). The extrapolation of Eq. (2) outside the range of measurements will introduce some uncertainty in the value of the diffusion coefficient but in the absence of additional information, this value was employed to obtain a qualitative estimate of the degree of coverage that could be expected.

From Eq. (2) and considering a diffusion time of 1 h (the annealing time), the expected coverage is given by $\Gamma(1\,\text{h}) = 6.53 \times 10^{-3} \times C^b$ (C^b in mol cm^{-3}). From the densities of Cu and Au [16], the alloy density was estimated at 17.77 g cm^{-3} assuming approximate ideal solution behaviour and therefore, a surface concentration of Pb can be estimated for a given concentration of impurity in the alloy. From the above, a 1 ppm concentration of Pb as impurity would result in a Pb coverage of 5.7×10^{-10} mol cm^{-2} or an atomic concentration of 3.5×10^{14} cm^{-2}. Considering a surface concentration of Au of 1.5×10^{15} cm^{-2} [17], these calculations predict a 23% surface coverage, very close to the value observed experimentally (~22%, see Fig. 3b). Although this is a very approximate calculation the similarity with the results calculated from the ARXPS data supports our assumptions.

It is interesting to carry out a qualitative estimate of the Gibbs energy of segregation of Pb (ΔG_S(Pb)) that the above results indicate and relate it to theoretical models. Considering the segregation process as an exchange of a host atom at the surface by a guest from the bulk, the equilibrium composition is given by [18,19]:

$$X^s_{Pb}/X^s_{Au} = X^b_{Pb}/X^b_{Au} \times \exp(-\Delta G_s(Pb)/RT) \quad (3)$$

where X^s and X^b refer to surface and bulk mol fractions, respectively. The Pb concentration specified in the base metals datasheet is less than 1 ppm. The measurement of the actual level of impurities in the materials employed to compare with this result presents great analytical difficulties. There is no reliable measurement of the saturation solid state solubility of Pb in Au. Owen and O'Donnell Roberts [20] could not detect any solubility using an X-ray method. The most reliable estimates are given in the compilation by Okamoto and Massalski [21] who indicated that the maximum solubility of Pb corresponds to $X^b_{Pb} < 0.04$ below 600 °C. Therefore, the estimate from Eq. (1) of 1 ppm ($X^b_{Pb} = 9.5 \times 10^{-7}$) for the concentration of Pb in the alloy is not unreasonable.

From these results, a value of ΔG_S(Pb) in the range of −60 kJ mol^{-1} can be estimated from Eq. (3), reflecting the strong driving force for Pb surface segregation. The physical meaning of ΔG_S has been the subject of much debate in the past. The classical macroscopic formalisms have been based on two important contributions, Gibbs energy of surface interactions and solute strain effects. The former was quantified using nearest neighbour interaction models whereas the latter relied on the calculation of strain effects caused by the introduction of the guest, with the resulting displacement in the position of the atoms in the host lattice. A necessary condition here is to assume relaxation of the lattice strain caused by the guest on transfer to the surface layer, which has to be modelled. The attraction (and limitations!) of this traditional approach is the use of macroscopic properties such as, for instance, the enthalpy of sublimation for the surface Gibbs energy calculations or the bulk modulus of the host and the shear modulus of the guest for strain energy estimates [18,22,23].

In order to quantify the driving force for the observed segregation we performed DFT calculations on Au(1 1 1) with different amounts of Pb (1/9, 1/4, and 1.0 ML Pb) either being adsorbed on the surface or by replacing Au atoms in the first, second, or third topmost layers. This provides information about the general segregation behaviour, even though multiple near-surface layers might be influenced by this segregation tendency (e.g., alternating decay of the enrichment by Pb).

Although the experimental studies were performed on $Au_{0.85}Cu_{0.15}$ bulk alloys, the theoretical studies were carried out for pure Au(1 1 1), the main alloy component. This approach was taken for simplicity since Au segregates preferentially to the surface in AuCu alloys, leading to a so-called Au-skin surface structure (see Fig. 3a) [6]. Thus, concentrating on the surface Au-skin layers, the use of a Au(1 1 1) surface is a reasonable compromise between a realistic surface model and computing resources. A more realistic model would require an in-depth investigation on the segregation behaviour of the Au, Cu, and Pb ternary system, with different bulk and surface compositions. This was, however, beyond the scope of the present work.

A comparison of the total energy of systems with the same composition already provides first insights in their stability. It was found that for a full Pb layer, the adsorption on the Au(1 1 1) surface is 0.16 and 0.27 eV/Pb-atom more stable than having Pb in the second or third surface layer respectively, i.e. below-surface absorption is not favourable. However, when considering lower coverages, absorption in the first layer becomes the preferred structure, while having Pb in the lower surface layers shows the same trend of decreasing stability as with a full Pb layer even though with higher energy differences. Here, having 1/4 ML Pb in the first surface layer is 0.74 and 1.00 eV/Pb more stable than having Pb in the second or third layers, respectively. Lowering the coverage to 1/9 ML, that can be considered as a zero-coverage limit, the segregation energy increases slightly to 1.00 and 1.16 eV/Pb, respectively. These calculations show that Pb is more likely to be at or near the surface of Au(1 1 1), a tendency that was also observed with ARXPS on the alloy investigated.

However, in order to compare the stability of systems with different surface compositions, the surface Gibbs energies rather than total energies must be analysed. Results from these calculations

Table 1
Surface Gibbs energies γ (in eV/surface-atom) for different amounts of Pb in different surface layers.

	Pb in layer	Coverage		
		1/9 ML	1/4 ML	1.0 ML
Adsorption	0	0.72	0.69	1.29
Absorption	1	0.70	0.61	1.28
	2	0.80	0.80	1.43
	Bulk	0.83	0.86	1.53

are shown in Table 1. Surface Gibbs energies should be lowest for the most stable configuration and the results in Table 1 indicate that the overall lowest value (i.e. highest stability) is obtained for 1/4 ML Pb in the first surface layer (γ = 0.61 eV/surface-atom), although adsorption on the surface is only 0.08 eV/surface-atom less stable. The next stable structure is with 1/9 ML Pb, where again absorption into the first surface layer is preferred. As expected, the least stable configuration is with a full Pb monolayer, which is certainly due to the relatively weak Pb–Pb interactions compared to those of Au–Au. From these calculations it can be concluded that Pb will indeed be segregated at the surface. The most stable configuration is obtained for a surface that contains roughly 1/4 ML Pb in the first layer, onto which additional Pb might be adsorbed. The greater stability of the 1/4 M Pb coverage derived from these calculations is in broad agreements with the ARXPS results and with predictions from the diffusion controlled adsorption model given by Eq. (1).

5. Conclusions

The results presented here are an example of the importance of low concentration of impurities in determining the surface composition of bulk alloys. DFT calculations clearly show that Pb impurity atoms have a strong tendency to accumulate near the surface (either adsorbed on the surface or absorbed in the first surface layer). Since annealing will enhance the system to assume its preferred structure and composition distribution, drastic changes in the catalytic behaviour would be expected for bulk samples. It is interesting to note, however, that the degree of surface contamination for nanoparticles will be strongly dependent on their size due to the availability of impurity atoms per cluster. In the example shown in this paper, if the alloy containing 1 ppm of Pb as impurity is present as nanoparticles of 5 nm diameter, on average 1 in 295 particles will contain a single atom of Pb and hence, will have a very small effect on the electrocatalytic properties of a nanoparticulate electrode a consequence of the confinement of Pb in the dispersed nanoparticle material. The influence of the impurities on electrocatalytic properties will depend, therefore, on the average size. So, even though a 1 ppm Pb content would appear to be a high concentration of poison for electrocatalytic reactions, this will have an almost undetectable effect for electrodes prepared with small nanoparticles.

Acknowledgements

This work was funded by the European Union, ELCAT Marie Curie Initial Training Network, Contract Nos. 214936-2 and 2008–2012. Further, T.J acknowledges support from the European Union through the ERC-Starting Grant THEOFUN. FJW acknowledges support from CONICET, UBA, and AGENCIA.

References

[1] J. Xu, T. White, P. Li, C. He, J. Yu, W. Yuan, Y.-F. Han, J. Am. Chem. Soc. 132 (2010) 10398–10406.
[2] J.S. Jirkovský, I. Panas, S. Romani, S. Ahlberg, D.J. Schiffrin, J. Phys. Chem. Lett. 3 (2012) 315–321.
[3] V.R. Stamenkovic, B. Fowler, B.S. Mun, G. Wang, P.N. Ross, C.A. Lucas, N.M. Markovic, Science 315 (2007) 493–497.
[4] C.L. Bracey, P.R. Ellis, G.J. Hutchings, Chem. Soc. Rev. 38 (2009) 2231–2243.
[5] E. Völker, F.J. Williams, E.J. Calvo, T. Jacob, D.J. Schiffrin, Phys. Chem. Chem. Phys. 14 (2012) 7448–7455.
[6] S. Venkatachalam, T. Jacob, Phys. Chem. Chem. Phys. 11 (2009) 3263–3270.
[7] T. Jacob, B.V. Merinov, W.A. Goddard III, Chem. Phys. Lett. 385 (2004) 374–377.
[8] M.D. Segall, P.J.D. Lindan, M.J. Probert, C.J. Pickard, P.J. Hasnip, J. Phys.: Condens. Mat. 14 (2002) 2717–2744.
[9] D. Vanderbilt, Phys. Rev. B 41 (1990) 7892–7895.
[10] G. Liu, K.A. Davis, D.C. Meier, P.S. Bagus, D.W. Goodman, G.W. Zajac, Phys. Rev. B 68 (2003) 035406.
[11] R.W. Paynter, An ARXPS primer, J. Electron Spectrosc. Relat. Phenom. 169 (2009) 1–9.
[12] G.C. Smith, A.K. Livesey, Surf. Interface Anal. 19 (1992) 175–180.
[13] A.J. Bard, L.R. Faulkner, second ed., John Wiley & Sons, New Jersey, 2001.
[14] H. Schopper, Z. Phys. 143 (1955) 93–117.
[15] H. Leidheiser Jr., Phys. Lett. 1 (1962) 39–40.
[16] J. Emsley, The Elements, Clarendon Press, Oxford, 1989.
[17] L.I. Berger, Fermi energy and related properties of metals, in: D.R. Lide (Ed.), CRC Handbook of Chemistry and Physics, Taylor and Francis, Boca Raton, 2007, pp. 12–209.
[18] F.F. Abraham, C.R. Brundle, J. Vac. Sci. Technol. 18 (1981) 506–519.
[19] D.C. Peacock, Appl. Surf. Sci. 27 (1986) 58–70.
[20] E.A. Owen, E.A. O'Donnell Roberts, J. Inst. Metals 71 (1945) 213–254.
[21] H. Okamoto, T.B. Massalski, Bull. Alloy Phase Diagrams 5 (1984) 276–284.
[22] P. Wynblatt, R.C. Ku, Surface Sci. 65 (1977) 511–531.
[23] S.H. Overbury, P.A. Bertrand, G.A. Somorjai, Chem. Rev. 75 (1975) 547.